

Electronic supplementary information (ESI)

**Octamethyl-substituted Pd (II) phthalocyanine with long carrier  
lifetime as dopant-free hole selective material for performance  
enhancement of perovskite solar cells**

Xiaolu Zheng, †, [a] Yulong Wang, †, [b] Jiahua Hu, [c] Guang Yang, [a] Zhen Guo, [d]  
Jianlong Xia, [c] Zongxiang Xu, \*, [b] Guojia Fang \*, [a]

[a] Key Lab of Artificial Micro- and Nano-Structures of Ministry of Education of  
China, School of Physics and Technology, Wuhan University, Wuhan 430072, P. R.  
China

\*Email: gjfang@whu.edu.cn

[b] Department of Chemistry, South University of Science and Technology of China,  
Shen Zhen, Guangdong 518055, P. R. China

\*Email: xu.zx@sustc.edu.cn

[c] School of Chemistry Chemical Engineering and Life Science, Wuhan University of  
Technology, No. 122 Luoshi Road, Wuhan 430070, P. R. China

[d] School of Materials Science and Engineering, Taiyuan University of Technology,  
Taiyuan Shanxi, 030024, P. R. China

† These authors contributed equally.

## Experimental Section

### Materials

Lead thiocyanate ( $\text{Pb}(\text{SCN})_2$ , 98%), [6,6]-phenyl-C61-butyric acid methyl ester (PCBM) and organic solvents were purchased from Sigma-Aldrich. 4,5-dimethylphthalonitrile was purchased from Shanghai Run Biotech. Lead (II) iodide ( $\text{PbI}_2$ , 99.8%), and Methylammonium iodide ( $\text{CH}_3\text{NH}_3\text{I}$ , MAI) were purchased from TCI. 2,2',7,7'-tetrakis(*N,N*-di-*p*-methoxy-phenylamine)-9,9'-spirobifluorene (spiro-OMeTAD, 99%) was purchased from ShenZhen Feiming Science and Technology Co., Ltd.. All chemicals were used as received without further purification unless specified otherwise. The Octal-methyl substituted Palladium (II) Phthalocyanine ( $\text{PdMe}_2\text{Pc}$ ) and Octal-methyl substituted Copper (II) Phthalocyanine ( $\text{CuMe}_2\text{Pc}$ ) was synthesized following the method we reported in our previous work<sup>[1]</sup>.

### Synthesis of Octal-methyl substituted Palladium (II) Phthalocyanine ( $\text{PdMe}_2\text{Pc}$ )

A mixture of 4,5-dimethylphthalonitrile (1.0 g, 6.4 mmol), palladium (II) chloride (0.28 g, 1.6 mmol), ammonium chloride (0.09g, 1.6 mmol), and *N,N*-dimethylformamide (5 ml) was put in a two-neck round bottom flask. The reaction mixture was stirred at 150 °C under argon overnight, and then allowed to cool down to room temperature. A 50 ml ethanol was introduced to resulting mixture to precipitate the product. The suspension was kept stirring for 5 min, and then filtered. The filter paper was washed with DI water, ethanol, and  $\text{CH}_2\text{Cl}_2$ . The solid was dried at 50 °C in oven and combined. To fulfill the requirements of electronic applications, the product was further purified by vacuum sublimation in a sublimation machine (Technol VDS-80) operated at 475 °C and  $\sim 5 \times 10^{-4}$  Pa. Elemental analysis calcd (%) for  $\text{C}_{40}\text{H}_{32}\text{PdN}_8$ : C, 65.71; H, 4.41; N, 15.33; found: C, 65.64; H, 4.28; N, 15.43. UV-Vis (1-chloronaphthalene):  $\lambda_{\text{max}} = 667$  nm. IR (KBr):  $\nu = 2970, 2914, 2875, 1620, 1508, 1462, 1406, 1354, 1309, 1176, 1143, 1114, 1035, 877, 815, 748, 721$   $\text{cm}^{-1}$ .

### Characterization of $\text{PdMe}_2\text{Pc}$

Density functional calculations (DFT) of the PdMe<sub>2</sub>Pc' geometric and electronic properties were conducted using the Gaussian 09 program package at the B3LYP/6-31G(d)\* level. Ultraviolet-visible (UV-vis) spectra of solution (in 1-chloronaphthalene) and solid thin films (60 nm) were obtained on a PerkinElmer Lambda750S spectrophotometer in a wavelength range of 300~800 nm at room temperature. Elemental analysis was performed by Vario MICRO analyzer. Thermogravimetric analysis (TGA) was recorded with a Discovery Thermogravimetric Analyzer. A few milligrams of solid sample were loaded on a platinum crucible, and the weight loss between 50 and 900°C at a rate of 10°C/min under a flowing N<sub>2</sub> stream was examined. Electrochemical measurements were carried out in a three-electrode glass cell at room temperature using an Autolab potentiostat. A commercially available glassy carbon disk, a Ag/AgCl electrode and a platinum wire were used as the working, reference and counter electrodes, respectively. A solution of 1-chloronaphthalene was used as the supporting electrolyte with ferrocenium/ferrocene redox couple (Fc/Fc<sup>+</sup>) as the internal standard. All the solutions were degassed with nitrogen for 10 min prior to measurement. The cyclic voltammetry (CV) was performed using a scan rate of 100 mV/s. The HOMO levels were estimated based on the onset oxidation potentials (E<sub>ox</sub>). Grazing incidence X-ray diffraction (GIXRD) patterns of the deposited films formed on FTO or Perovskite substrates were recorded using a Smartlab 9 kW diffractometer with a Göbel mirror attachment. Irradiation of the parallel Cu K $\alpha$ <sub>1,2</sub> X-ray beam was fixed at a grazing incident angle of 1.000°( $\theta$ ) and the detector was independently moved to collect the diffraction data in 2 $\theta$  range of 4–30° with a step-size of 0.02° (2 $\theta$ ) at a fixed speed of ca. 5 s/step. Noted that the thin film samples of bare PdMe<sub>2</sub>Pc and PCBM/Perovskite/PdMe<sub>2</sub>Pc were deposited on FTO glass following the same fabrication procedures as we described below. Transient absorption (TA) spectra were measured by a commercial femtosecond pump–probe system (Transient Absorption Spectrometer, Newport Corporation). Laser pulses at 1040 nm with <400 fs duration was generated by a 200 kHz amplified laser system (Spirit 1040-8-SHG, Newport Corporation). The probe beam was a white light continuum beam spanning 500-950 nm spectral region, which is created by focusing a fraction of the 1040 nm fundamental

output onto a YAG crystal. The rest of the output light was used to generate the pump pulses at 520 nm by a second harmonic generation, and the induced absorption changes ( $\Delta A$ ) were recorded as functions of both wavelength and time. Pump–probe delay is controlled by a translational stage. And the samples thickness for TA measurement are determined to be 180 nm using the spectroscopic ellipsometry (FTS2-S4C-3D, Taylor Hobson, UK). The hole mobility ( $\mu_h$ ) of PdMe<sub>2</sub>Pc was measured using a HP4155A semiconductor parameter analyzer (Yokogawa HewlettPackard, Tokyo, Japan), the  $\mu_h$  was extracted by fitting the  $J$ - $V$  curves of a balanced device according to the modified Mott–Gurney equation  $J = 9\epsilon_0\epsilon_r\mu V^2/8d^3$ <sup>[2]</sup>. where  $J$  is the current density,  $\epsilon_0$  is the permittivity of free space,  $\epsilon_r$  is the relative permittivity,  $\mu$  is the zero-field mobility,  $V$  is the applied voltage, and  $d$  is the thickness of active layer (in there the thickness of PdMe<sub>2</sub>Pc was 300 nm). The device structure is FTO/SnO<sub>2</sub>/Perovskite/PdMe<sub>2</sub>Pc/Au, where the perovskite layer was used as a template. Similar testing method was also employed to detect the  $\mu_h$  of CuMe<sub>2</sub>Pc in our previous study<sup>[1]</sup>.

### **Device Fabrication and Characterization**

Perovskite solar cells (PSCs) were fabricated with the structure of FTO/SnO<sub>2</sub>/PCBM/Perovskite/PdMe<sub>2</sub>Pc/Au. The FTO glasses we used there were patterned and with a sheet resistance of 14  $\Omega/\square$ . They were pre-cleaned in an ultrasonic bath of deionized water, acetone, and ethanol, and then treated in an Ultraviolet-ozone chamber (Novascan Company, USA) for 15 min. SnO<sub>2</sub> electron selective layers (ESLs) were prepared by spin-coating the solution of 0.1 M SnCl<sub>2</sub>·2H<sub>2</sub>O dissolved in ethanol on FTO substrate with a spin rate of 2000 rpm for 30 s, and then annealed on a hotplate in air at 185°C for 1 hour. Details were described in our previous work<sup>[3]</sup>. A thin layer of PCBM was then spin-coated on SnO<sub>2</sub> substrate with a spin rate of 2000 rpm and baked in glove-box at 100°C for 10 min. The PCBM solutions were prepared by dissolving 15 mg PCBM in 1 ml dichlorobenzene. Perovskite absorber layers were deposited on ESLs by a solvent engineering method<sup>[4]</sup>. The precursor was prepared by dissolving 461 mg PbI<sub>2</sub>, 159 mg MAI and 8 mg Pb(SCN)<sub>2</sub> in 723  $\mu$ L N,N-dimethylformamid (DMF) and 81  $\mu$ L dimethyl sulfoxide (DMSO). The hole selective

layers (HSLs) of PdMe<sub>2</sub>Pc or CuMe<sub>2</sub>Pc were grown by thermal evaporation under a vacuum of  $\sim 1 \times 10^{-6}$  Torr, and the layer thickness was monitored in-situ using quartz crystal monitors during deposition. Finally, gold electrode was thermally evaporated on top of the HSL to complete the device. The active area of the cells was 0.09 cm<sup>2</sup>.

The top-view and cross-section images of the PSCs with PdMe<sub>2</sub>Pc HSL were observed using a high-resolution field emission scanning electron microscope (FE-SEM) (JSM 6700F, Japan). The current density-voltage ( $J$ - $V$ ) properties were characterized on a CHI 660D electrochemical workstation (Shanghai Chenhua Instruments, China) with a standard ABET Sun 2000 Solar Simulator. A standard silicon solar cell was used to adjust the light intensity to 1 sun condition (100 mW cm<sup>-2</sup> and AM 1.5G). The corresponding external quantum efficiency (EQE) was measured by a QE-R 3011 system (Enli Technology Co. Ltd. China) in the range of 300~800 nm wavelength. Absorbance spectra were measured by an UV-vis spectrophotometer (CARY5000, Varian, Australia). The crystalline structure of Perovskite was characterized by an X-ray diffractometer (XRD) (D8 Advance, Bruker AXS, Germany), using Cu K $\alpha$  radiation ( $\lambda=0.1542$  nm) at 40 kV and 40 mA. The steady-state photoluminescence (PL) measurements were carried out under a 488 nm laser at room temperature, and the emission signal was collected via a Micro Raman Spectroscopy system (LabRam HR, HORIBA Jobin Yvon, France). The trap-filled limit voltages ( $V_{TFL}$ ) of different MPCs were obtained from the dark current-voltage ( $I$ - $V$ ) analysis. The device structure used there is FTO/PEDOT:PSS/perovskite /PdMe<sub>2</sub>Pc or CuMe<sub>2</sub>Pc/Au. The linear relation at the beginning of  $I$ - $V$  curves indicates an ohmic response of devices. And when the bias voltage exceeds the intersection (marked as  $V_{TFL}$ ), the current increases nonlinearly, suggesting that the trap states in perovskite layer are completely filled. The trap-filled limit voltage ( $V_{TFL}$ ) was determined by the trap-state density:  $V_{TFL} = en_t L^2 / 2\epsilon\epsilon_0$ , where  $e$  is the elementary charge of the electron,  $L$  is the thickness of the perovskite film,  $\epsilon$  is the relative dielectric constant of perovskite,  $\epsilon_0$  is the vacuum permittivity, and  $n_t$  is the trap-state density. In there the  $L$  is estimated at 400 nm from the cross-section SEM image, and  $\epsilon$  is 28.8 according to the references<sup>[5, 6]</sup>. Topographic images of the thin film samples were recorded by atomic force microscopy (AFM) (SPM-9500J3,

Shimadzu, Japan). The contact angle measurement of perovskite, spiro-OMeTAD, and PdMe<sub>2</sub>Pc surface were recorded by Drop Shape Analyzer (DSA 25S, KRUSS). For long-term stability test the devices (PdMe<sub>2</sub>Pc and spiro-OMeTAD) were unsealed and stored in ambient air and under dark conditions. More specifically, we stored them in a dry box with 30 ± 5% relative humidity and temperature of 25 ± 5 °C. The devices were periodically taking out to test, and the testing conditions are room temperature and relative humidity of 50%. And for the comparison between PdMe<sub>2</sub>Pc and CuMe<sub>2</sub>Pc the devices were stored outside the dry box and suffering a room light and fluctuant relative humidity (from 40% to 100%). The devices were periodically testing their respective UV-Vis spectra using a SHIMADZU UVmini-1280 spectrophotometer in a wavelength range of 300~800 nm.

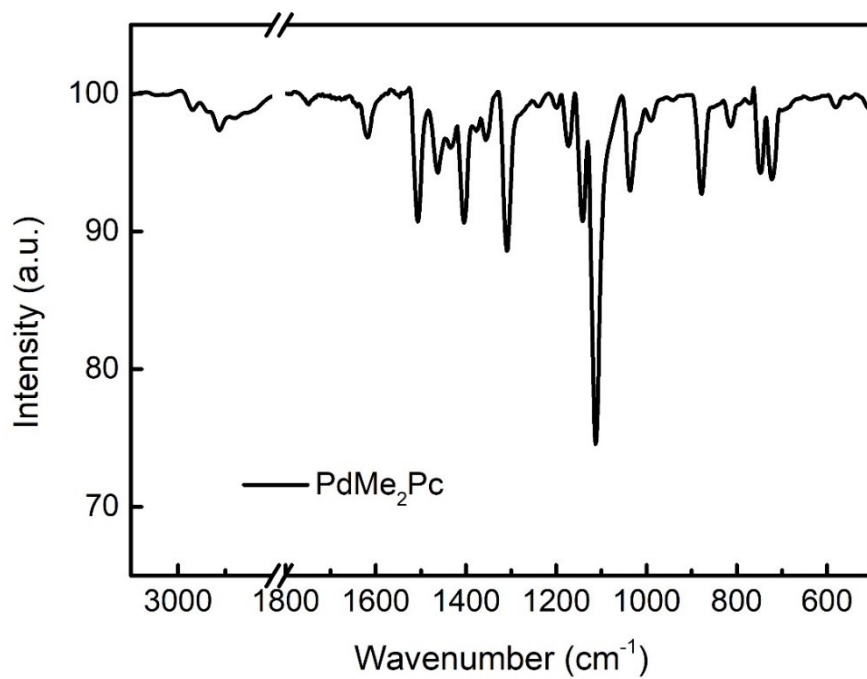


**Figure S1.** Infrared spectrum of PdMe<sub>2</sub>Pc.

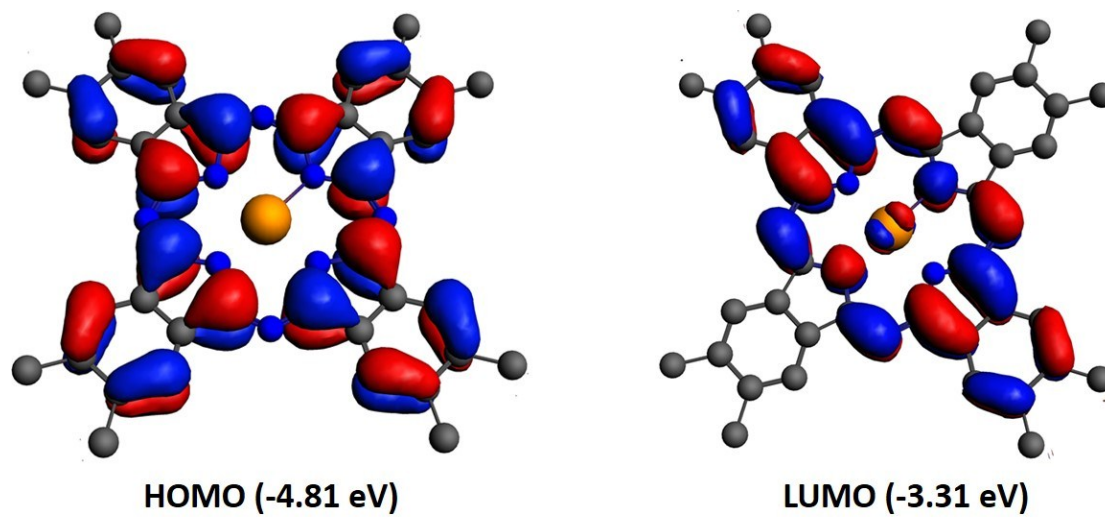


**Figure S2.** Molecular orbital maps of Kohn-Sham HOMO and LUMO of PdMe<sub>2</sub>Pc.

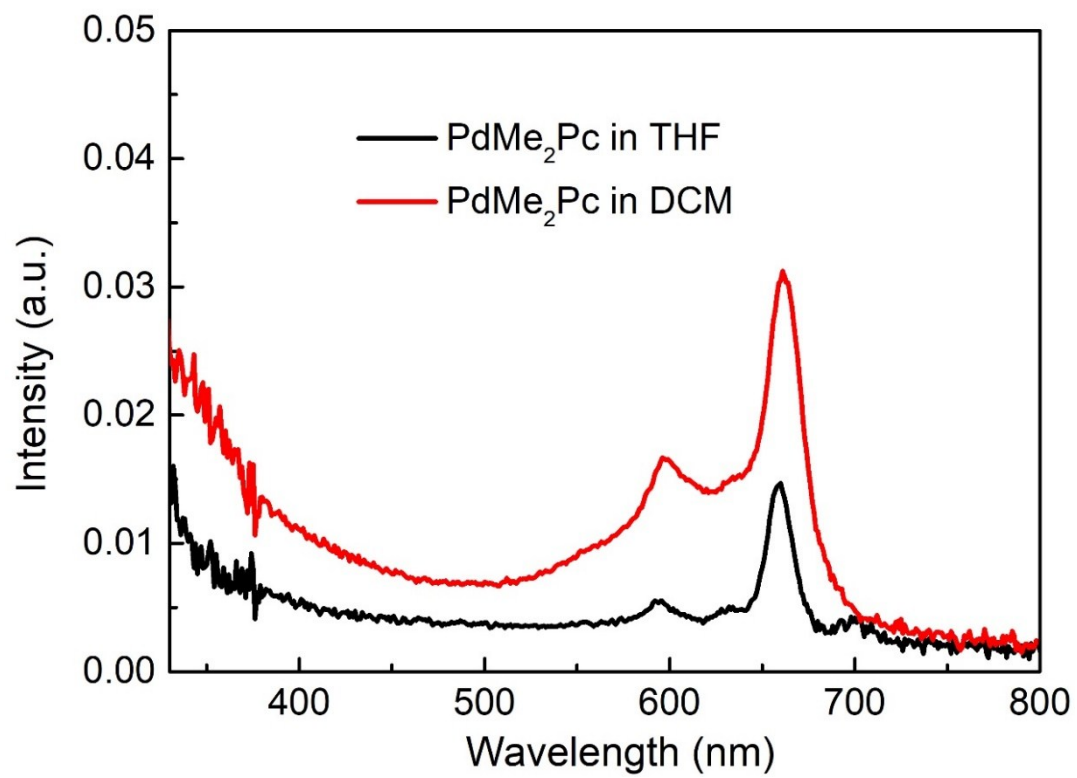


**Figure S3.** UV-vis absorption spectra of PdMe<sub>2</sub>Pc tested in Tetrahydrofuran (THF) and dichloromethane (DCM).

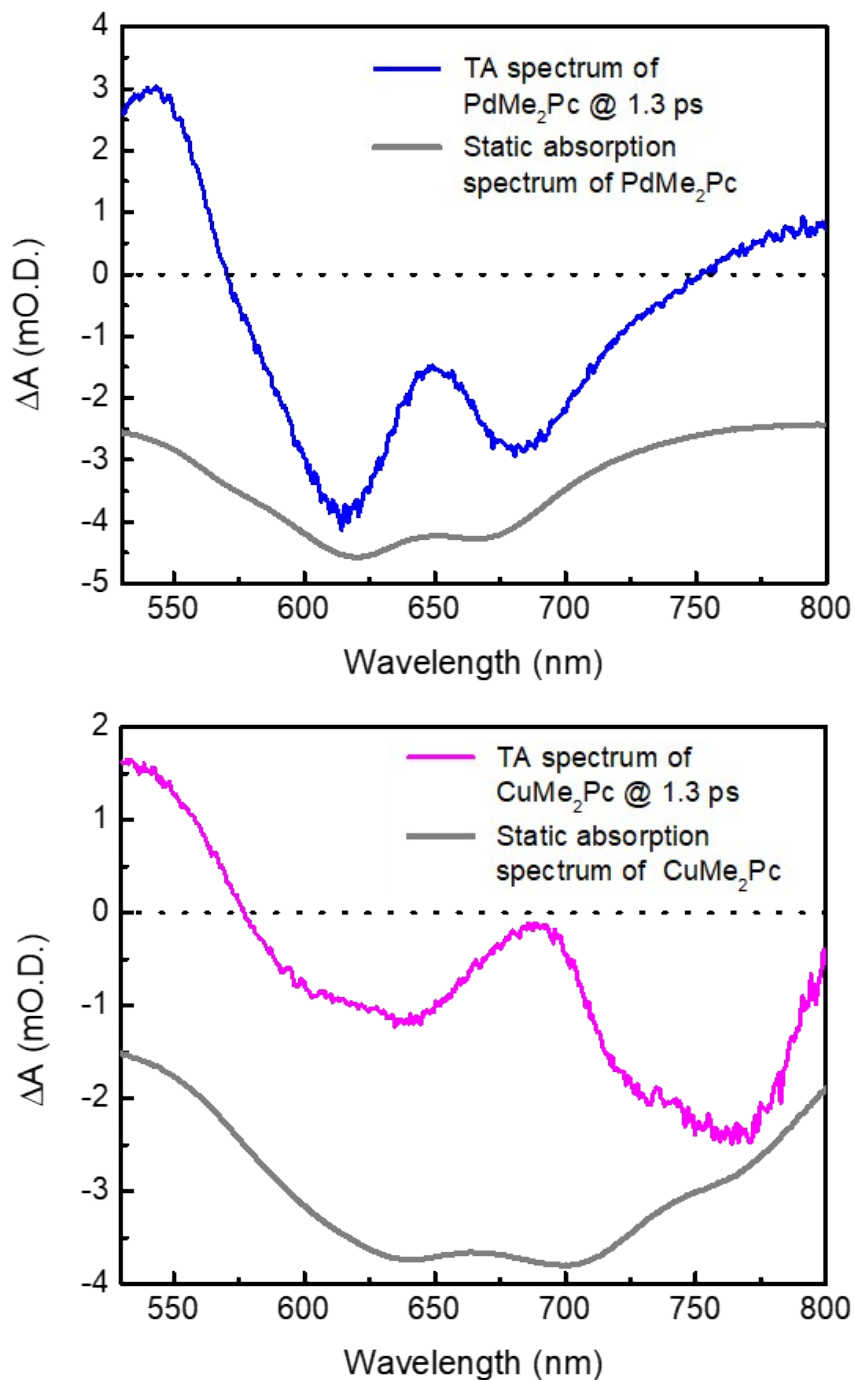


**Figure S4.** Transient absorption and UV-vis static absorption spectra of PdMe<sub>2</sub>Pc (upper panel) and CuMe<sub>2</sub>Pc (lower panel) tested as thin films. The TA spectra were choosing at 1.3 ps when the signal reached the maximum, and the inverted ground state absorption spectra (artificially scaled for viewing) are shown as a thick gray line for comparison

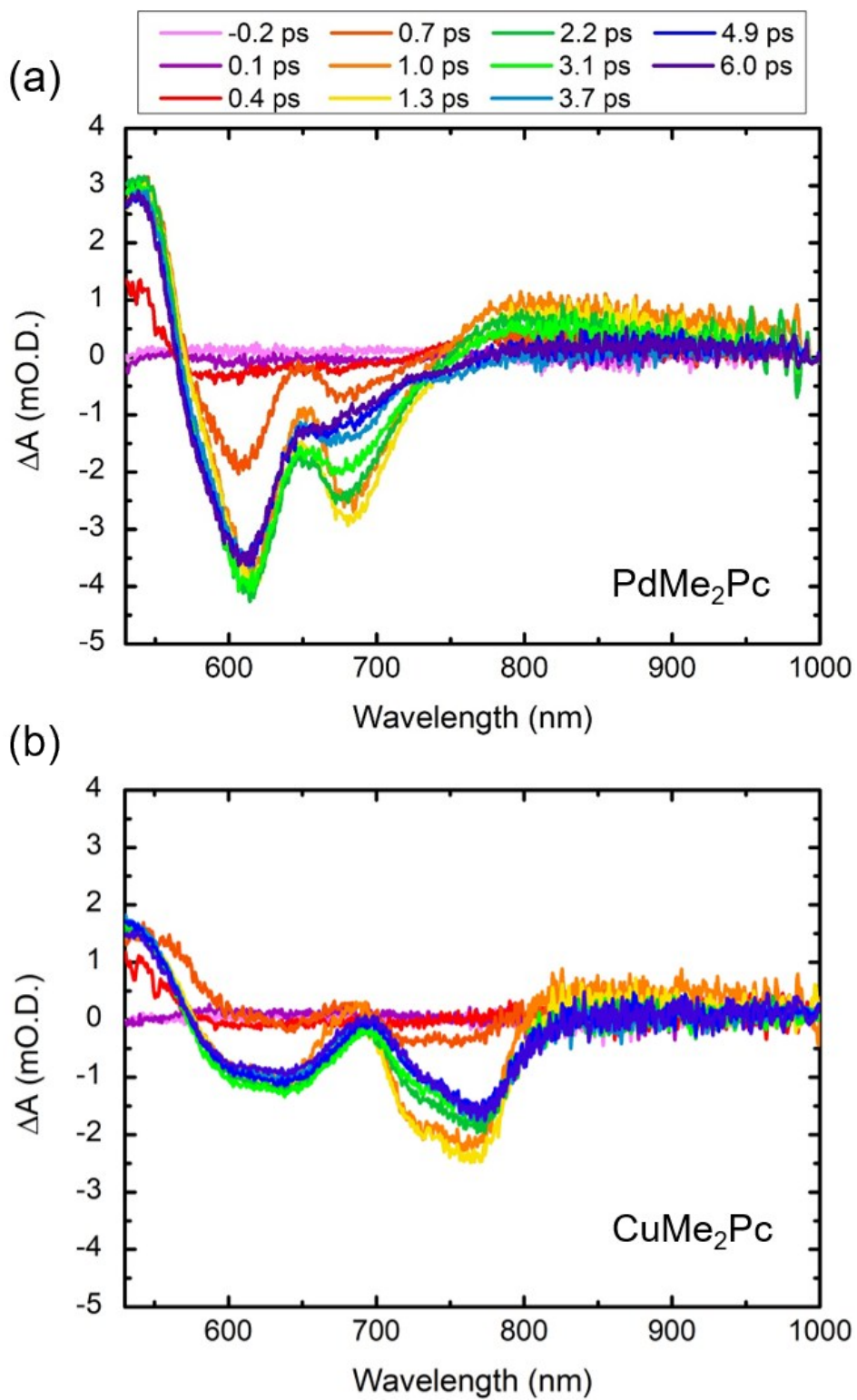


**Figure S5.** Transient absorption spectra of vapor deposited (a) PdMe<sub>2</sub>Pc and (b) CuMe<sub>2</sub>Pc (ca. 180 nm) excited at 520 nm in the first 6 picoseconds. The iridescence indicates the spectral evolution (from red to blue).

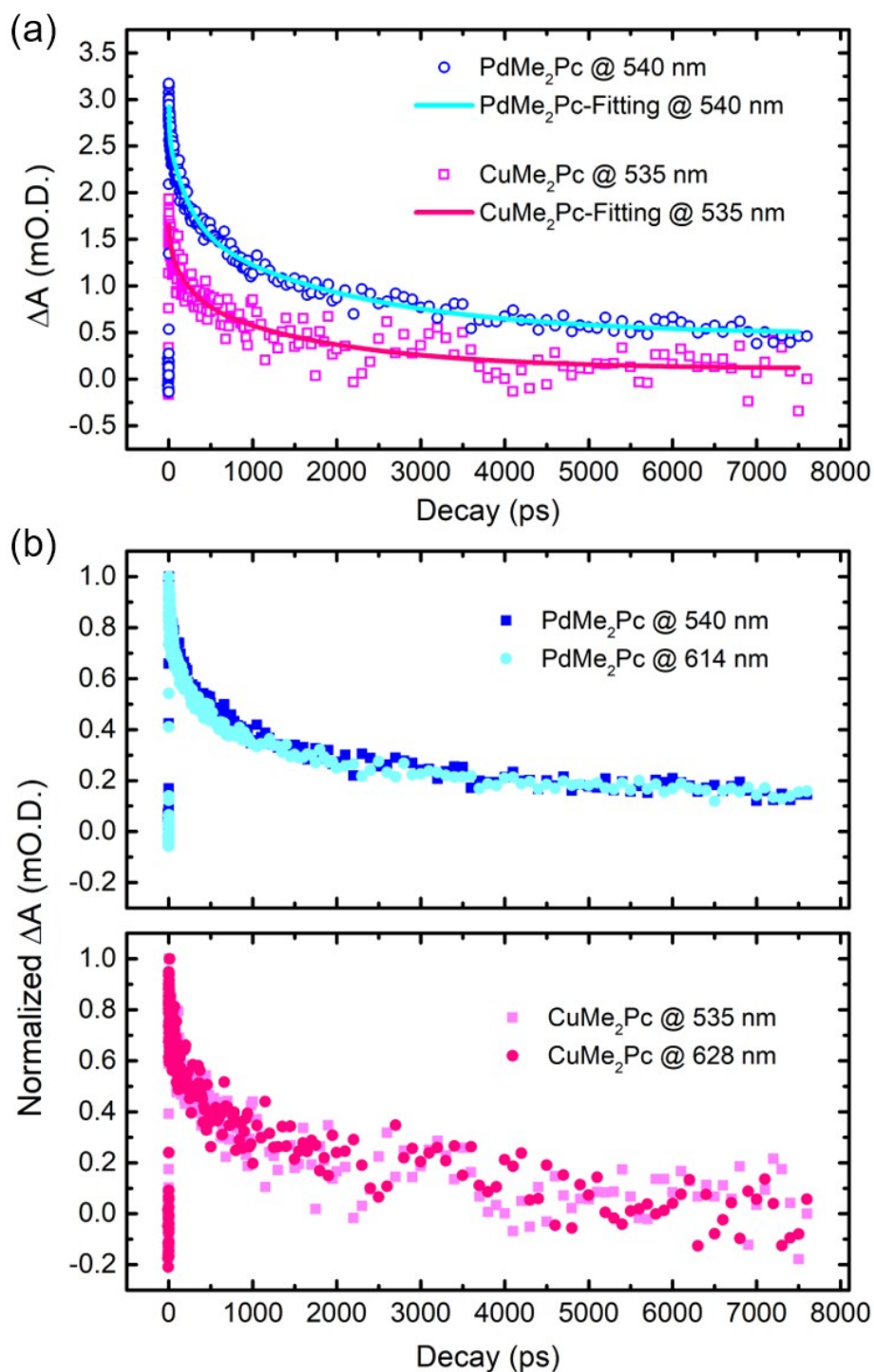


**Figure S6.** (a) Kinetic traces of PdMe<sub>2</sub>Pc at 614 nm and CuMe<sub>2</sub>Pc at 628 nm. (b) Time profiles comparison of PdMe<sub>2</sub>Pc at 540 nm and 614 nm (upper panel), and of CuMe<sub>2</sub>Pc at 535 nm and 628 nm (lower panel). Noted the normalized Y axis at (b) panel.

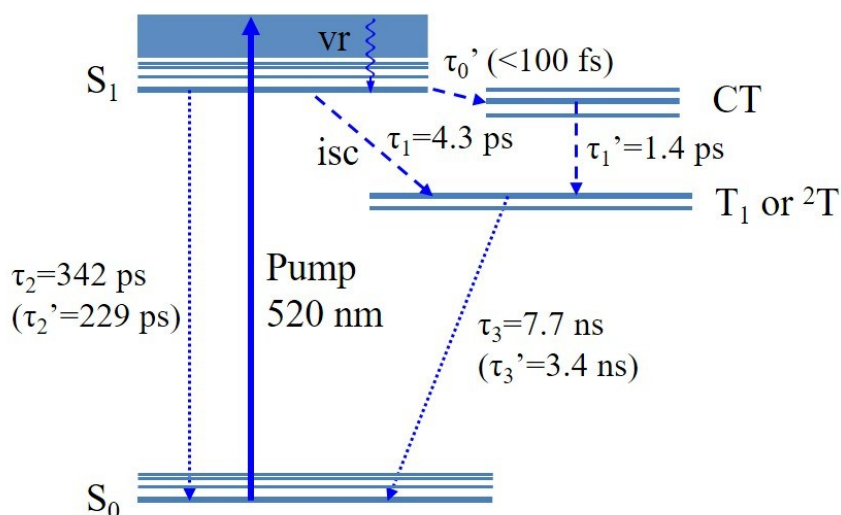


**Figure S7.** Schematic diagram of the energy relaxation dynamics of PdMe<sub>2</sub>Pc and CuMe<sub>2</sub>Pc after photoexcitation to the S<sub>1</sub> excited state. vr and isc represent the vibrational relaxation and intersystem crossing processes, respectively. The  $\tau_1$ ,  $\tau_2$ ,  $\tau_3$  corresponding to the lifetime of PdMe<sub>2</sub>Pc, and  $\tau_1'$ ,  $\tau_2'$ ,  $\tau_3'$  to that of CuMe<sub>2</sub>Pc.

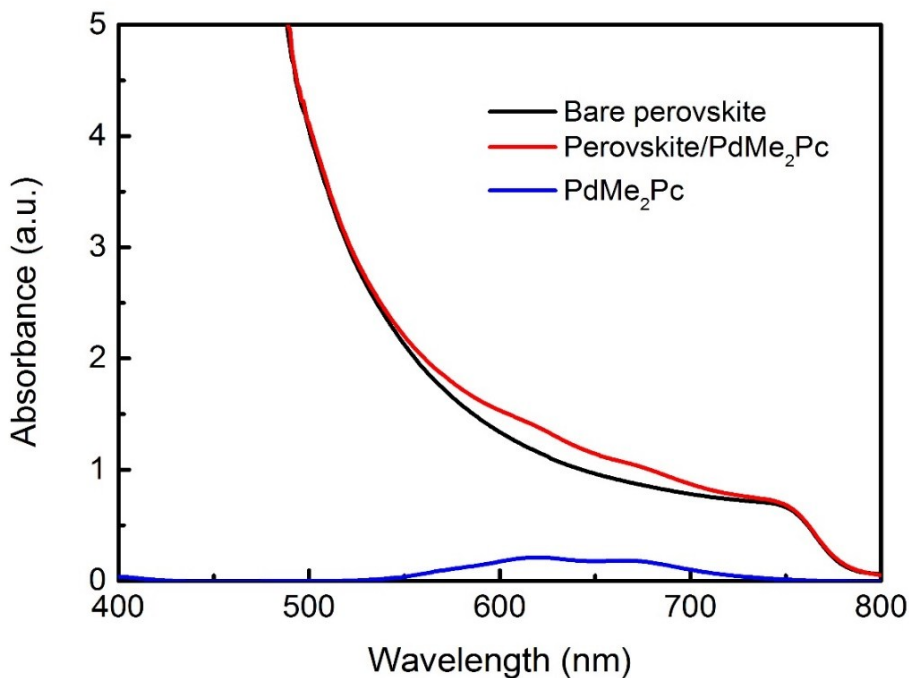


**Figure S8.** UV-Vis absorbance spectra of FTO/PdMe<sub>2</sub>Pc, FTO/perovskite, and FTO/perovskite/PdMe<sub>2</sub>Pc (60 nm).

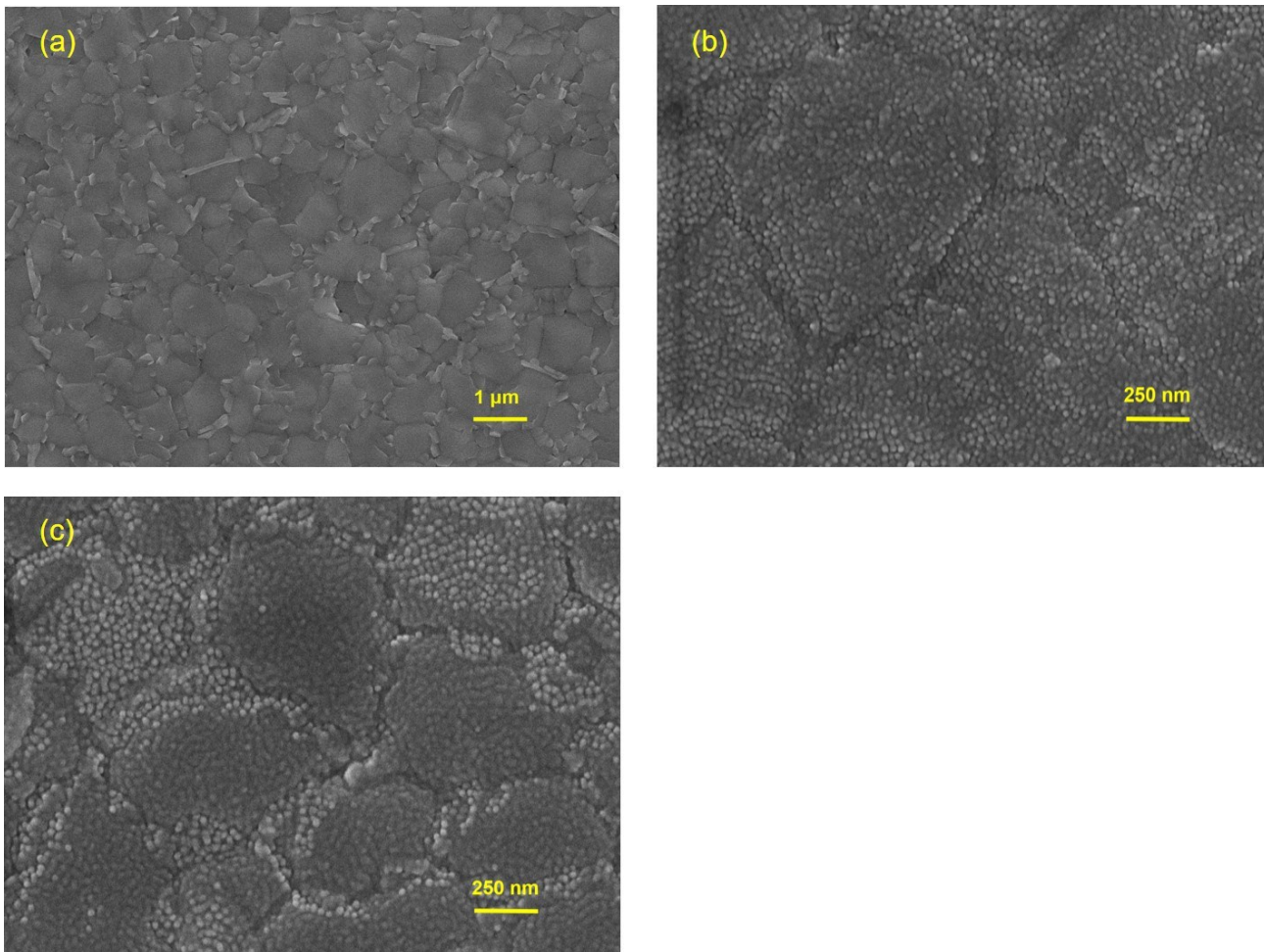


**Figure S9.** Top-view SEM image of (a) perovskite film deposited on FTO/SnO<sub>2</sub>/PCBM substrate, (b) PdMe<sub>2</sub>Pc film deposited on FTO/SnO<sub>2</sub>/PCBM/perovskite substrate, (c) CuMe<sub>2</sub>Pc film deposited on FTO/SnO<sub>2</sub>/PCBM/ perovskite substrate. The thickness of PdMe<sub>2</sub>Pc and CuMe<sub>2</sub>Pc both are 60 nm. Noted the difference of scale bar.

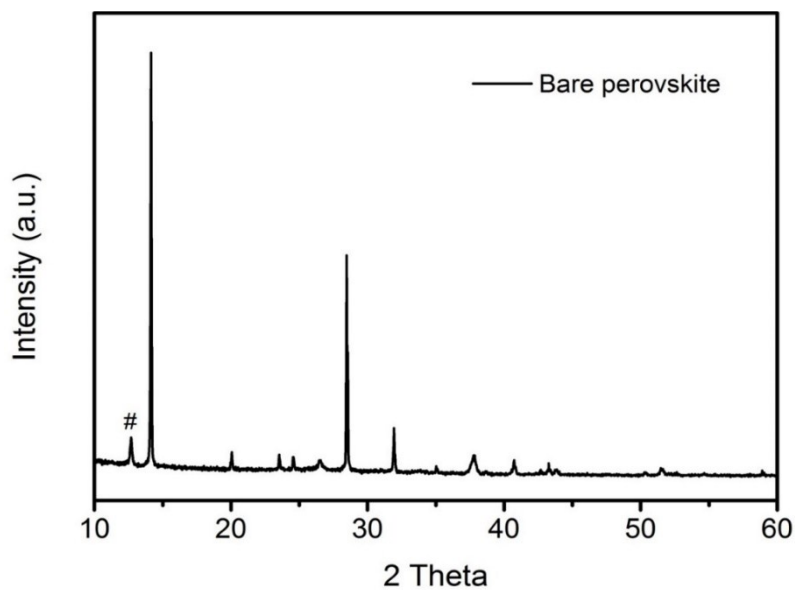


**Figure S10.** XRD pattern of a bare perovskite film. The two strong peaks at  $14.12^\circ$  and  $28.46^\circ$  are attributed to the (110) and (220) planes of  $\text{CH}_3\text{NH}_3\text{PbI}_3$ , and the small peak that located at  $12.66^\circ$  (marked with #) is corresponding to the (001) plane of  $\text{PbI}_2$ .

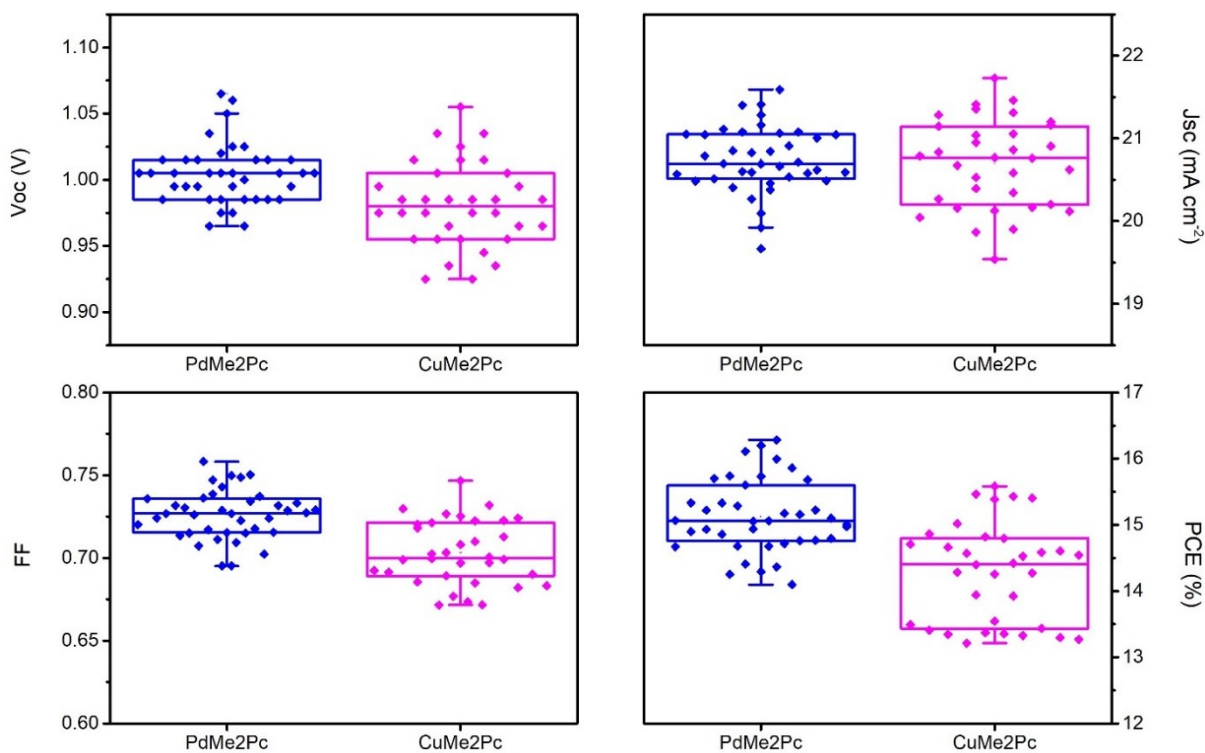


**Figure S11.** Photovoltaic parameters statistics of 39 PdMe<sub>2</sub>Pc and 34 CuMe<sub>2</sub>Pc based devices as collected from four batch.

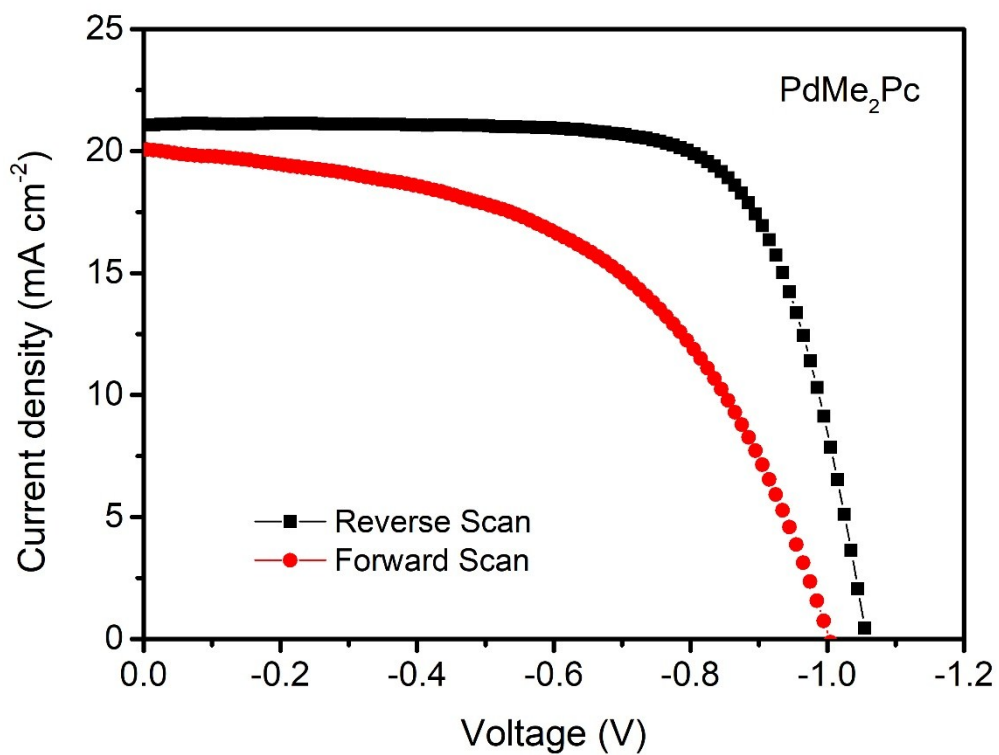


**Figure S12.**  $J$ - $V$  hysteresis of the device based on PdMe<sub>2</sub>Pc HSL.

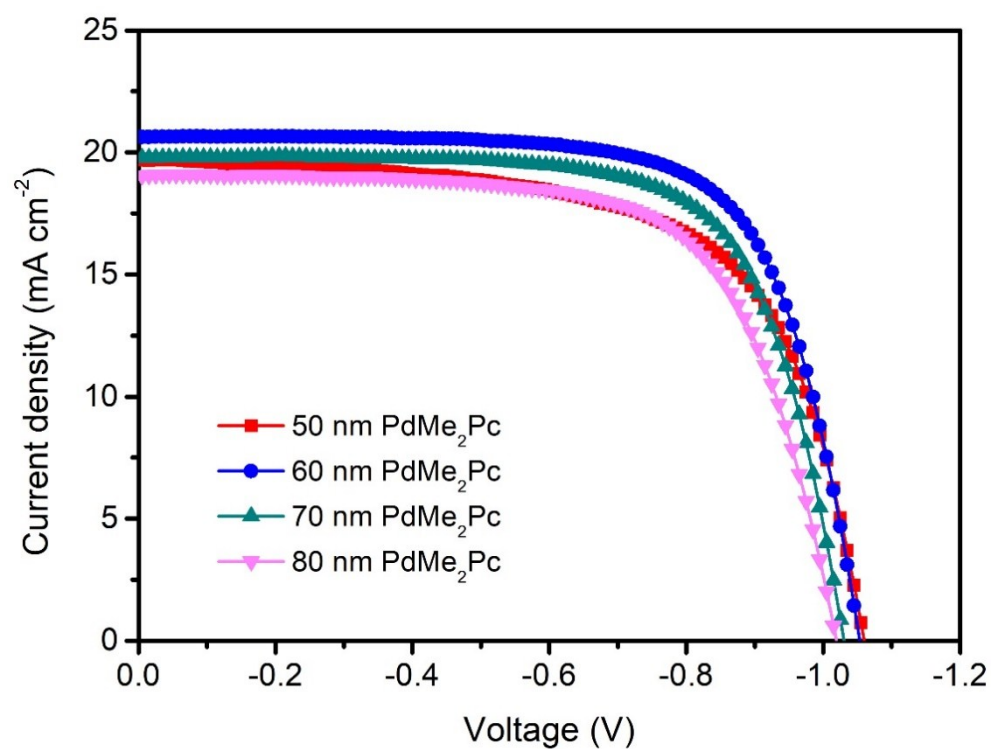


**Figure S13.**  $J$ - $V$  curves of the devices based on PdMe<sub>2</sub>Pc HSL with varied PdMe<sub>2</sub>Pc thicknesses.

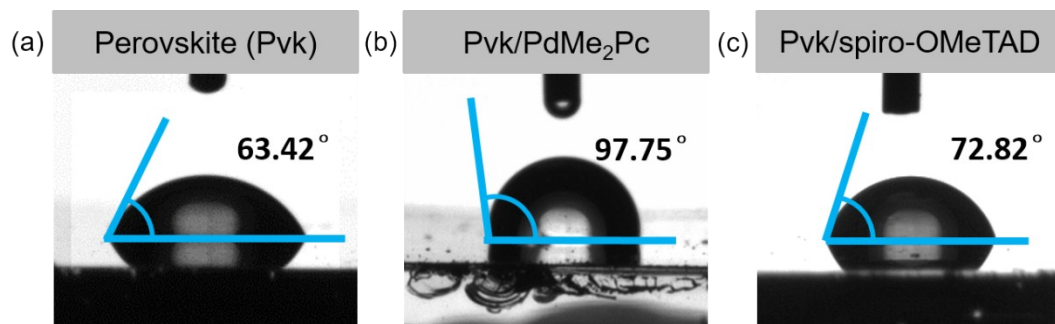


**Figure S14.** Static contact angles of water droplets on the surface of (a) bare perovskite, (b) perovskite/PdMe<sub>2</sub>Pc and (c) perovskite/spiro-OMeTAD.

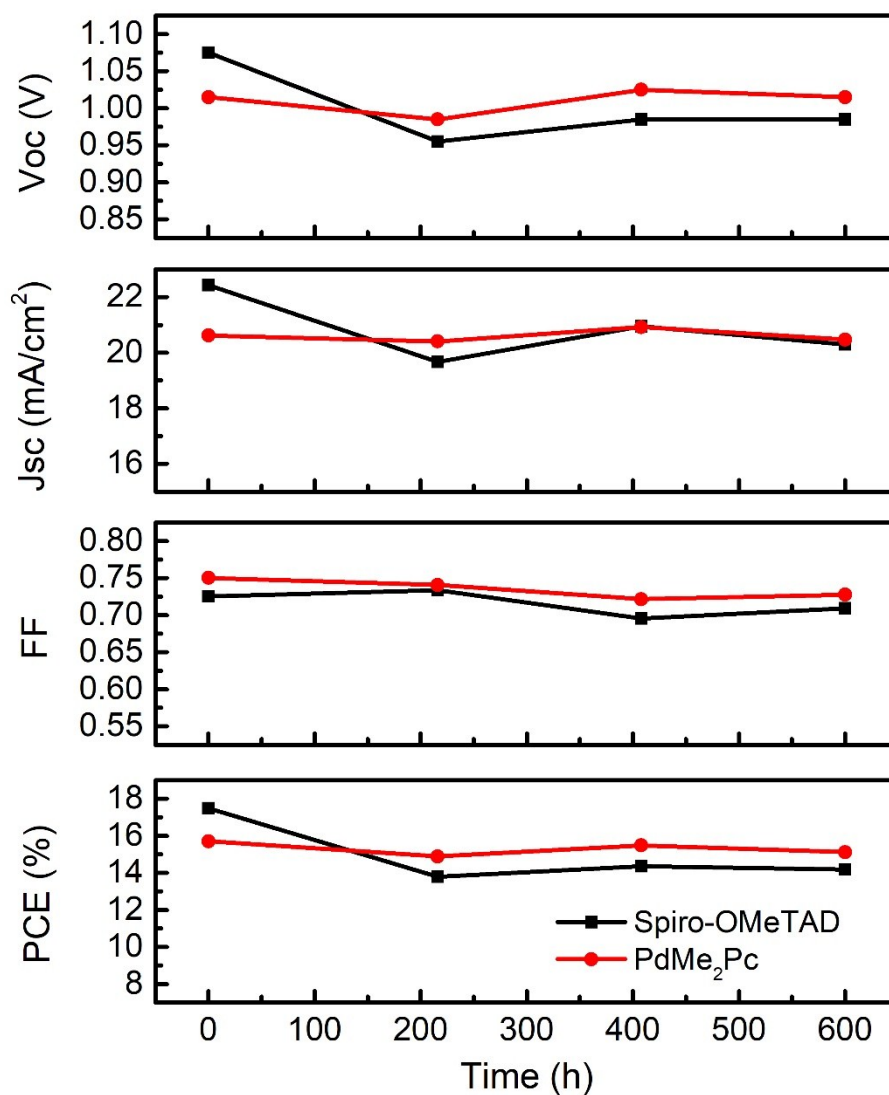


**Figure S15.** Long-term stability of the PSCs with PbMe<sub>2</sub>Pc (red circle) and spiro-OMeTAD (black square) HSLs.

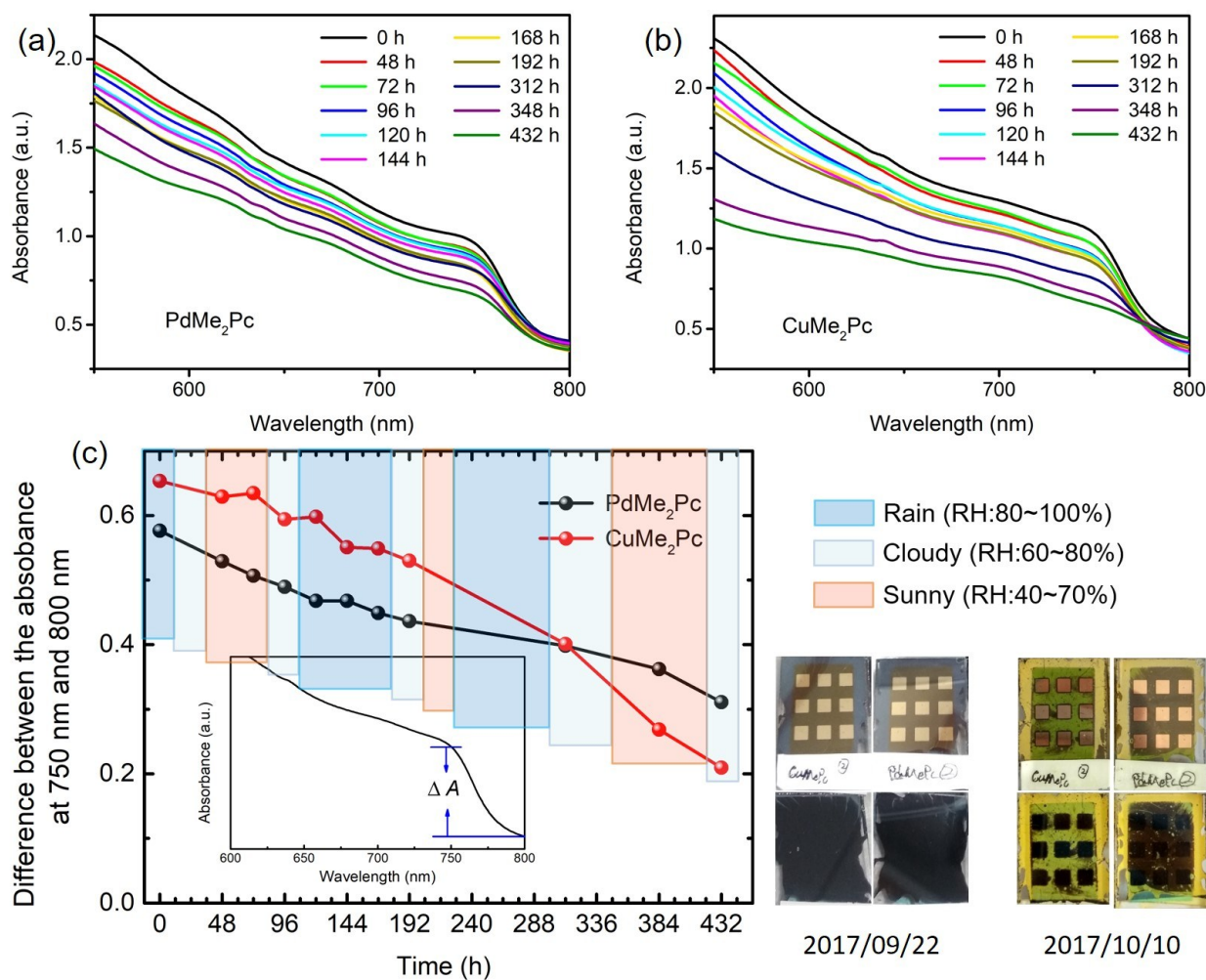


**Figure S16.** The absorption spectra of (a) PdMe<sub>2</sub>Pc- and (b) CuMe<sub>2</sub>Pc-based devices as a function of storing time. (c) The corresponding changes of the difference between the absorbance at 750 nm and 800 nm, and the photographs of these two devices at the beginning and end of this test are also shown in the bottom right corner.

**Table S1.** Summary of the optical and electrochemical parameters of PdMe<sub>2</sub>Pc.

Compound	$\lambda_{\max}$		$E_{\text{onset}}^{\text{ox}}$ [V]	HOMO <sup>c</sup> [eV]	LUMO <sup>d</sup> [eV]	$E_g$ <sup>b</sup> [eV]
	Solution <sup>a</sup>	Film				
PdMe <sub>2</sub> Pc	667	685	0.76	-5.11	-3.30	1.81

<sup>a</sup> All these CV and UV were tested in 1-chloronaphthalene solution;

<sup>b</sup> The band gap ( $E_g$ ) value was extracted from the film's UV spectrum;

<sup>c</sup> The HOMO level was calculated based on the respective onsets of oxidation potentials of the compounds via the equation:  $\text{HOMO} = -e (E_{\text{onset}}^{\text{ox}} + 4.8 - 0.45)$

<sup>d</sup> The LUMO level was calculated via the equation:  $\text{LUMO} = \text{HOMO} + E_g$

**Table S2.** Summary of the fitted decay lifetime factors and their corresponding transition process of PdMe<sub>2</sub>Pc and CuMe<sub>2</sub>Pc.

HSL		$\tau_1$ <sup>a</sup>	$\tau_2$	$\tau_3$
PdMe <sub>2</sub> Pc	Lifetime	4.3 ps	342 ps	7.7 ns
	Transition	$S_1 \rightarrow T_1$	$S_1 \rightarrow S_0$	$T_1 \rightarrow S_0$
CuMe <sub>2</sub> Pc	Lifetime	1.4 ps	229 ps	3.4 ns
	Transition	${}^2S_1 \rightarrow {}^2CT \rightarrow {}^2T$	$S_1 \rightarrow S_0$	${}^2T \rightarrow S_0$

<sup>a</sup> The kinetic traces were fitted by the triexponential function:  $y = A_1 * \exp(-x/\tau_1) + A_2 * (-x/\tau_2) + A_3 * (-x/\tau_3)$ , where  $A_1$ ,  $A_2$  and  $A_3$  are the prefactors,  $\tau_1$ ,  $\tau_2$  and  $\tau_3$  are the lifetimes of the different decay component, respectively.

**Table S3.** Summary of photovoltaic parameters of PSCs employing HSL of PdMe<sub>2</sub>Pc and CuMe<sub>2</sub>Pc.

HSL	$V_{oc}$ [V]	$J_{sc}$ [mA/cm <sup>2</sup> ]	FF	PCE [%]	$R_s$ <sup>a</sup> [ $\Omega$ cm <sup>2</sup> ]	$A$ <sup>a</sup>
PdMe <sub>2</sub> Pc	1.00±0.03	20.74±0.40	0.73±0.01	15.13±0.55	2.31±0.43	2.35±0.24
CuMe <sub>2</sub> Pc	0.98±0.03	20.69±0.53	0.70±0.02	14.28±0.75	2.33±0.56	2.67±0.39

<sup>a</sup> The  $R_s$  and  $A$  are calculated according to the diode equation<sup>[7]</sup>:  $-dV/dJ = AK_B T(J_{sc} - J)^{-1}e^{-1} + R_s$ , where  $A$  is ideality factor,  $K_B$  is Boltzmann constant,  $T$  is the absolute temperature, and  $e$  is the elementary charge.

**Table S4.**  $J$ - $V$  parameters of PSCs with different PdMe<sub>2</sub>Pc thicknesses.

	$V_{oc}$ [V]	$J_{sc}$ [mA cm <sup>-2</sup> ]	FF	PCE [%]	$R_s$ <sup>b</sup> [ $\Omega$ cm <sup>2</sup> ]	$A$ <sup>b</sup>
50 nm PdMe <sub>2</sub> Pc <sup>a</sup>	1.055	19.69	0.65	13.45	1.86	3.34
60 nm PdMe <sub>2</sub> Pc	1.055	20.63	0.71	15.44	1.99	2.84
70 nm PdMe <sub>2</sub> Pc	1.035	19.78	0.70	14.42	2.46	2.80
80 nm PdMe <sub>2</sub> Pc	1.015	19.06	0.68	13.16	2.16	3.46

<sup>a</sup> The thickness of PdMe<sub>2</sub>Pc was monitored with a quartz crystal thickness monitor

<sup>b</sup> The  $R_s$  and  $A$  are calculated according to the diode equation<sup>[7]</sup> we mentioned above.

## References

1. G. Yang, Y. Wang, J. Xu, H. Lei, C. Chen, H. Shan, X. Liu, Z. Xu and G. Fang, *Nano Energy*, 2017, **31**, 322-30.
2. W. Ke, G. Fang, Q. Liu, L. Xiong, P. Qin, H. Tao, J. Wang, H. Lei, B. Li, J. Wan, G. Yang and Y. Yan, *J. Am. Chem. Soc.*, 2015, **137**, 6730-3.
3. W. Ke, C. Xiao, C. Wang, B. Saparov, H. S. Duan, D. Zhao, Z. Xiao, P. Schulz, S. P. Harvey, W. Liao, W. Meng, Y. Yu, A. J. Cimaroli, C. S. Jiang, K. Zhu, M. Al-Jassim, G. Fang, D. B. Mitzi and Y. Yan, *Adv. Mater.*, 2016, **28**, 5214-21.
4. G. G. Malliaras, J. R. Salem, P. J. Brock and C. Scott, *Phys. Rev. B*, 1998, **58**, 13411-4.
5. D. Yang, R. Yang, X. Ren, X. Zhu, Z. Yang, C. Li and S. Liu, *Adv Mater*, 2016, **28**, 5206-13.
6. Z. Chen, G. Yang, X. Zheng, H. Lei, C. Chen, J. Ma, H. Wang and G. Fang, *J. Power Sources*, 2017, **351**, 123-9
7. J. Shi, J. Dong, S. Lv, Y. Xu, L. Zhu, J. Xiao, X. Xu, H. Wu, D. Li, Y. Luo and Q. Meng, *Appl. Phys. Lett.*, 2014, **104**, 063901.